UNIVERSITY OF CALIFORNIA,
IRVINE

Deformation mechanisms in Bimodal structured Copper: A molecular dynamics study

THESIS

submitted in partial satisfaction of the requirements
for the degree of

MASTER OF SCIENCE

in Material Science and Engineering

by

Han Wang

Thesis Committee:
Associate Professor Penghui Cao, Chair
Associate Professor Tim Rupert
Assistant Professor William Bowman

2021

DEDICATION

To

my parents and friends

in recognition of their worth

TABLE OF CONTENTS

LIST OF FIGURES

ACKNOWLEDGEMENTS

I would like to express the deepest appreciation to my committee chair, Professor Penghui Cao Irvine, who has the attitude and the substance of a genius and induced me to the world of Molecular Dynamics simulation. Without his help, the thesis would never have the chance to be finished.

I would like to thank my committee members, Professor Tim Rupert and Professor William Bowman, whose work demonstrated to me the beauty of computational and experimental research.

In addition, a thank you to all my friends for the meaningful discussions and to the staffs work at Starbuck and Boba shops that always prepare good drinks that helps me gain energy.

ABSTRACT OF THE THESIS

Deformation mechanisms in Bimodal structured Copper: A molecular dynamics study

by

Han Wang

Master of Science in Material Science and Engineering

University of California, Irvine, 2021

Associate Professor Penghui Cao, Chair

[Bimodal structure has become a promising way to alleviate the famous strength and ductility trade-off in metals. For conventional nanocrystalline metals, strong strength softening follows after Hall-Petch effect withing the continuous decrease of grain size. In our study, we conducted molecular dynamics (MD) study and discovered that as the decrease of small grain size in bimodal nanograined structures, the softening rate of inverse Hall-Petch effect is suppressed. With the increasing number of small grains around the large grains, the plasticity of large grains is enhanced, and they also undergo less intergranular grain boundary sliding and migration leading to the increasing stress of large grains. The discovery of this process could be beneficial to designing bimodal nanograined structures with desired ductility and strength.]

INTRODUCTION

It is known that, with the decreasing grain size, the strength of polycrystalline metals will be enhanced first, however, after the critical threshold value it will then experience a drastic downfall[1]. This strength softening effect due to the continuous decreasing grain size is called inverse Hall-Petch effect[2], and it is governed by grain boundary activities such as stress-induced intergranular sliding[3], dislocation-grain boundary interaction[4], and shear-coupled boundary migration[5][6].

Over the years, the new emergent heterogeneous structures[7], such as gradient[8], bimodal[9], multimodal structures[10], have drew the public's attention together with its unique mechanical properties. Due to their unprecedented grain size distribution, the famous strength-ductility-trade-off can thereby be alleviated. It not only exhibits great mechanical behaviors but also provides a way of achieving the desired properties by manipulating the parameters of structure. Bimodal nanograined (BNG) Copper, with coarse grains embedded in ultrafine grains, was first introduced in 2002 by Yinmin etc.[9]. Because of its inhomogeneous microstructure, the strain hardening mechanism that stabilize the tensile deformation is induced, leading to a high strength and ductility at the same time reaching 65 % elongation to failure and 30 % uniform elongation. Fascinated by the exceptional properties, the bimodal structure was found applicable to other metals, such as Nickel[10], Aluminum[11] , and Titanium[12]. All the nanograined metals with bimodal structure obtained superior mechanical properties than that of homogeneous nanograined (HNG) metals. Even so, the most intrinsic underlying mechanisms of the bimodal structure are still not well understood. However, the previous experimental studies are suggesting that

the grain size ratio plays an extremely fundamental role to the mechanical behavior of bimodal[13][9].

As a result, we performed massively parallel atomistic simulations for BNG Cu with varying grain size ratios and then compared the results with HNG Cu, a material which has been well studied in both experiments and simulations[9][14][15]. It is shown that, with the decreasing small grain size, the strength of large grains is enhanced, thus it leads to the alleviation of the strength softening effect on BNG Cu. By analyzing the deformation process, it is found that with the decreasing size of the grains around the large grains, more dislocations are generated within the large grains. What's more, we also observed less intergranular grain boundary sliding and migration among large grains. This triggers multiple dislocation slip systems, twinning, and the formation of stacking faults, indicating an improved plasticity of large grains. The discovery of this process is beneficial to understanding the underlying deformation mechanisms of heterogeneous structures and guiding the design of BNG metals.

Chapter 1 Literature Review

In this chapter, the background of the heterogenous structured metals and metallic glass will be introduced. The progress made in recent years regarding the aforementioned topics will be discussed.

1. Heterogenous Structured Metals

Hetero-structured metals are the emerging material research topic. Due to the unique heterogeneity of the grain size distribution, structures such as bimodal structure, gradient structure and lamella structure tend to exhibit superior mechanical and physical properties, especially towards strength-ductility synergy, that are not attainable by conventional homo-structured metals .

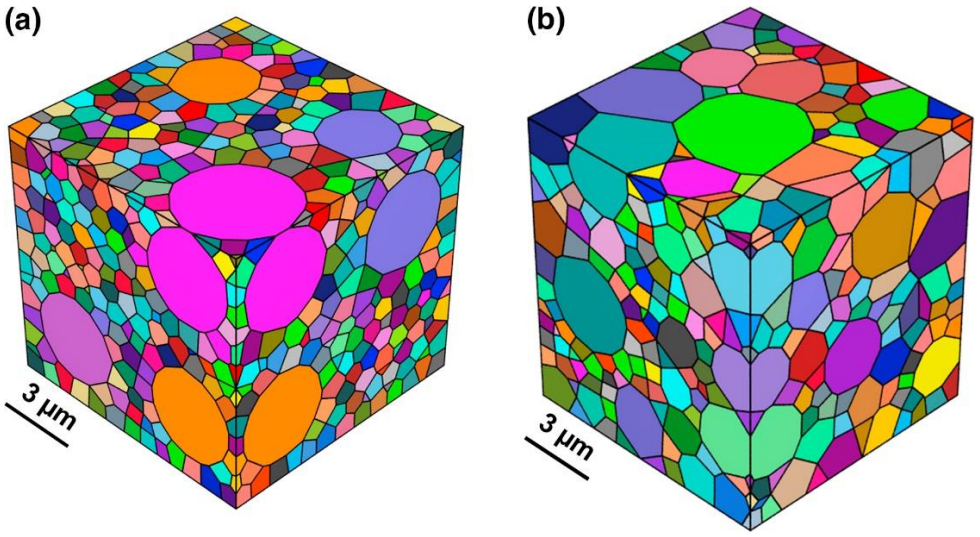

Figure 1.1 | Structure models of heterogenous grains with controllable grain size and distribution. (a) A bimodal grained structured with ~50 vol% grains of size of 1 1 mm and 50 vol% grains of 6 mm. (b) A trans-modal grained structure distribution. (a) A bimodal grained structure with ?50 vol% grains of size with a uniform distribution of grain sizes in between 1 mm and 6 mm. Grain is colored according to its orientation assigned randomly.

In 2002, Yinmin Wang et al[9]. described a thermomechanical treatment of Cu that results in a bimodal grain size distribution, with micrometer-sized grains embedded inside

a matrix of nanocrystalline and ultrafine (<300 nm) grain. Their processing starts by rolling Cu at liquid nitrogen temperature to a high value of percentage cold work and then annealing. Rolling at liquid nitrogen can suppress dynamic recovery of the grains and achieve the ultrafine grain matrix, and annealing allows the recovery of micrometer-sized grains, together forming a bimodal grain size distribution. The inhomogeneous microstructure induces strain hardening mechanisms that stabilize the tensile deformation, leading to a high tensile ductility, 65% elongation to failure, and 30% uniform elongation. J.Bach and et al[14]. obtained bimodal copper by equal channel angular pressing (ECAP) followed by annealing at 125℃ or, respectively, at 140℃ subsequent to the ECAP-process, and then systematically studies the deformation mechanisms and strain rate sensitivity. It was concluded that the bimodality is the deterministic factor of the dominant deformation mechanism and the strain-rate sensitivity. In the ultrafine grain, thermally activated annihilation of dislocation at the grain boundaries govern the mechanical behavior. However, for the coarse grain, the annihilation of dislocation at the interface of coarsened grains to the surrounding ultrafine-grained matrix dominated the mechanical behavior. Ivan Lonardelli and et al[16]. reported the plastic strain recovery deformation behavior in bulk nanocrystalline-ultrafine aluminum. In their study, spark plasma sintering at 620℃ is applied to produce the bimodal nano-crystalline-ultrafine Al from consolidation of nanostructured powders, and then it was investigated under in situ compressive loading using high-energy synchrotron X-ray diffraction. After one loading-unloading cycle, to 2% strain, it is found that the reversible peak is hereby broadened within the nanocrystalline grain volume and that tensile residual stress reached 80 MPa within the ultrafine grain volume. Upon unloading, they also discovered recovery of 12% of the plastic strain. With the

higher applied deformations to 4%, the recovery would increase up to 28%. The residual stresses induced by the inhomogeneous strains act as a driving force to drive dislocations back to the grain boundaries where they originated.

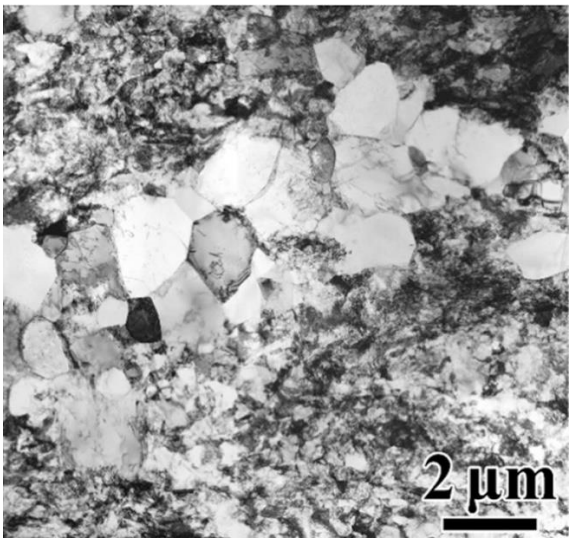

Figure 1.2 | TEM image of Ti with heterogeneous lamella structure, showing a lamella of recrystallized grains in between two lamellae of ultra-fine grains.

Knowing how the heterogeneity can attribute the unprecedented mechanical behavior, Xiaolei Wu and et al[17]. reported a heterogeneous lamella structure in Ti produced by asymmetric rolling and partial recrystallization that can alleviate the strength and ductility trade-off. It is also found that the unusual high strength is obtained with the assistance of high back stress developed from heterogeneous yielding, whereas the high ductility is attributed to back-stress hardening and dislocation hardening. In addition, Junjie Sun and et al[18]. studied a novel process to obtain lamella structured low-carbon steel with bimodal grain size distribution and its corresponding mechanical property. By applying a two-step warm rolling and subsequently annealing the desired structure is then successfully produced, of which the yield strength and tensile strength are increased by 87.4% and 35% respectively when compared with initial coarse grain steel. It is concluded that the enhanced

strength mainly comes from the ultrafine grain strengthening, and the reasonable ductility can be attributed to both the bimodal grain size and the lamellar structure, which can increase the work hardening rate by the accumulation of geometrically necessary dislocations in their vicinity.

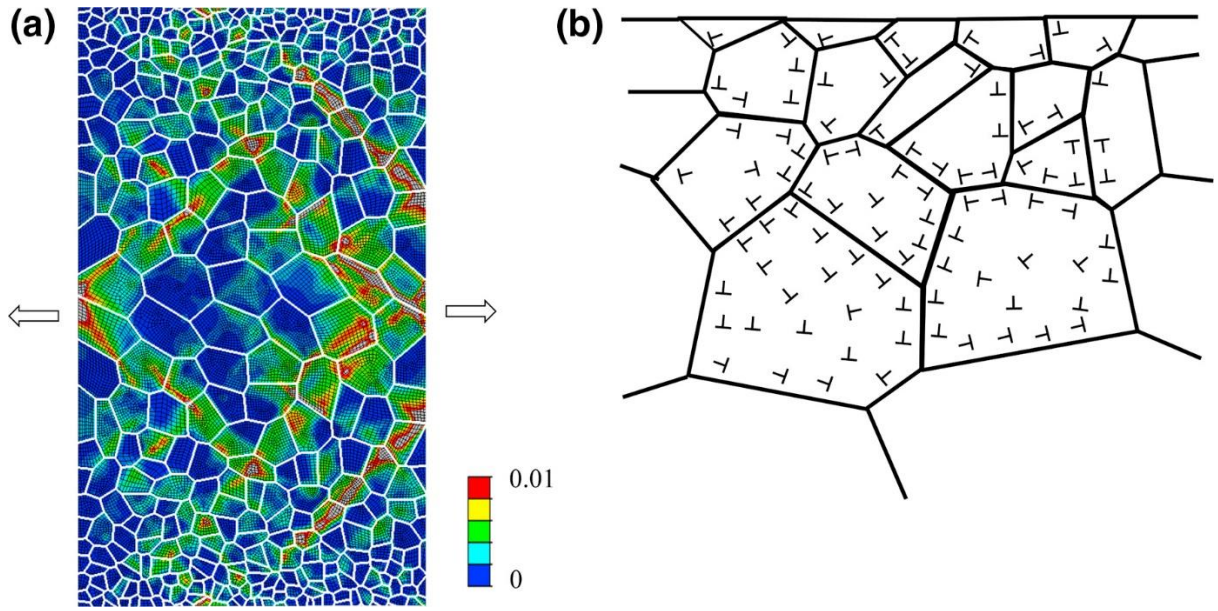

Figure 1.3 | Modeling of plastic strain gradients imposed by gradient nano-grains in Cu. (a) A finite element crystal plasticity model of quasi-two-dimensional structure of columnar nano-grains was constructed with a continuous spatial gradient of grain sizes linearly varying from ~20 nm in the top/bottom surface layer to ~110 nm in the central region. The sample is pulled under axial tension along the horizontal direction and color by the plastic strains. (b) Schematic illustration of a gradient variation of the density of geometrically necessary dislocations in a gradient nano-grained structure.

Besides bimodal and lamella structured metals, nanomaterials with gradient structure, in which the grain size increases from nanoscale at the surface to coarse-grained in the core, also can lead to outstanding mechanical properties. By applying surface plastic deformation onto a bulk coarse-grained metal, K. Lu et al[19]. were able to generate the distinctive gradient microstructure from the strain gradient. The extraordinary tensile ductility of the gradient nanograined surface layer, which is several times stronger than the coarse-grained structure, leads to a strength-ductility synergy. T. H. Fang and et al[20]. also

reported the extraordinary intrinsic tensile plasticity in gradient nano-grained copper. They conducted a surface mechanical grinding treatment (SMGT) for preparing a nano-grained (NG) Cu film with a spatial gradient in grain size, which achieved a large tensile plasticity and revealed a different governing deformation mechanism. It is concluded that a mechanically driven grain boundary migration process with a substantial concomitant grain growth dominated plastic deformation of the gradient NG structure.

Unlike the conventional mechanical testing methods that are not able to trace the structure changes with respect to the deformation process, Molecular Dynamics (MD) Simulation has become a very efficient way to study the deformation behavior and mechanical properties. Penghui Cao[8] performed massively parallel atomistic simulations in gradient nanograined Cu and homogeneous nanograined Cu. It is found that the strongest size, which lies between the Hall-Petch effect and inverse Hall-Petch effect, can be tuned by tailoring grain size gradient, and raising in the gradient shifts in the size toward the smaller value. In addition, the essential deformation mechanisms are also analyzed. The decrease of strongest size is mainly induced by mitigation of grain boundary-mediated softening and processes together with the enhanced intragranular plastic deformation. In addition, Zhi Zeng and et al[21]. studied the gradient mechanical behavior in gradient nano-grain copper by a crystal plasticity finite element modal, which revealed that both gradient stress and gradient plastic strain in the cross section of GNC copper subjected to axial tension. These spatial gradients are from the progressive yielding of the gradient grains under an overall uniform deformation.

In conclusion, the new emergent heterogeneous structures, such as gradient , bimodal, multimodal structures, have drew the public's attention together with its unique

mechanical properties. Due to their unprecedented grain size distribution, the famous strength-ductility-trade-off can thereby be alleviated. It not only exhibits great mechanical behaviors but also provides a way of achieving the desired properties by manipulating the parameters of structure. However, the most intrinsic underlying deformation mechanisms of the heterogeneous structure are still not well understood, especially lack of the support from computation method for bimodal structured metals. As a result, in this study, we performed massively parallel atomistic simulations in bimodal structured copper and revealed its deformation mechanisms.

Chapter 2 Deformation Behavior of Bimodal Structured Copper

In this chapter, the detailed study regarding bimodal structured copper will be introduced, including simulation modal, method, simulation results and conclusions.

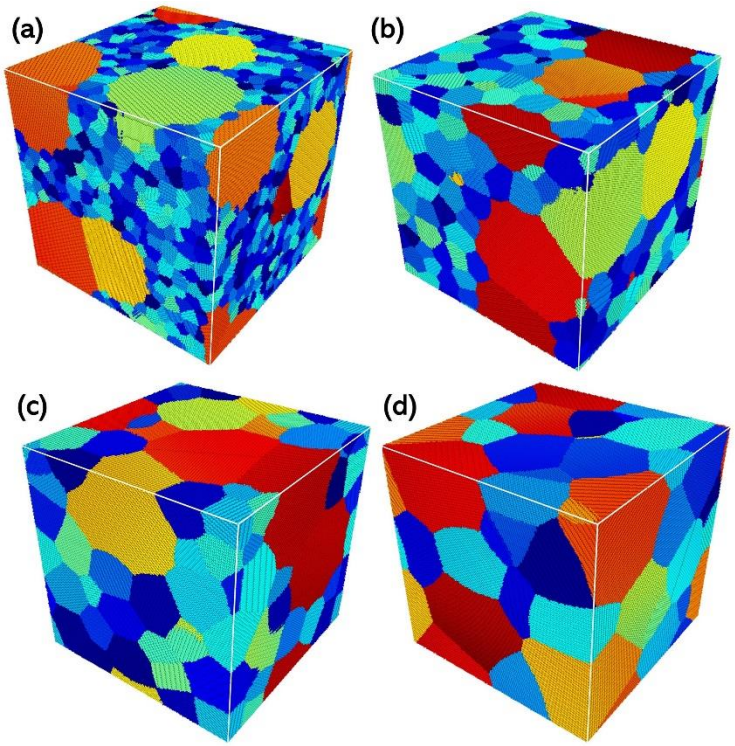

Figure 2.1 | Simulation modal of bimodal structured Cu with varying small grain sizes. (a) 3 nm, (b) 6 nm, (c) 10 nm, and (d) 14 nm.

1. Simulation modal

The bimodal nanograined structures (BNG) with a box size of 40 nm × 40 nm × 40 nm were generated with Dream.3D[22], which is a 3D structure builder that allows users to construct customized workflows to build synthetic microstructures. To study BNG small grain size *d* effect, the size of large grain is fixed to 20 nm with the small grain size ranging from 2 nm to 15 nm, and both large grains and small grains take 50% of the structure volume. There are approximately 5.5×10^6 atoms in each BNG, 7650 grains in the BNG with smallest small grain size, and 27 grains in the BNG with the largest small gain size. A series of

homogeneous structures with the same box size and varying grain sizes are also generated as comparison. All the grains are randomly orientated. Figure 2.1 shows the typical Bimodal structured Cu with varying small grain sizes from 3 nm to 14 nm.

2. Method

In this study , we performed massively parallel atomistic simulations in BNG Cu with varying grain size ratios and then compared the results with homogeneous nanograined Cu, a material which has been well studied in both experiments and simulations. For Molecular Dynamics (MD) simulations, the small gains and the large grains were set as two different atom groups to analyze the mechanical behaviors individually. An embedded-atom method (EAM) potential[23] was set as the interatomic interaction of Cu atoms, and all the simulations were conducted at constant 300 K using Nosé-Hoover thermo-stat[24][25]. The boundary conditions along *x*, *y*, and *z* directions are all periodic. The structures were first annealed at 300 K and then a uniaxial tensile strain was applied to the *y* direction. The components of kinetic energy tensor and the virial tensor from pairwise interaction were considered during the calculations of stress. All samples are deformed at a constant strain rate of 5×10^8 s^{-1}, and the stress in other directions perpendicular to tensile deformation was controlled at zero stress using Berendsen barostat[26]. Later on, different strain rates from 5×10^7 s^{-1} to 1×10^{10} s^{-1} were performed on the BNG with 14 nm small grain size and 20 nm HNG to study the strain rate effect under the same condition.

3. Simulation Results

The calculated average plastic flow stresses from 10% to 20% applied strain for each BNG structure are shown in Figure 2.2c. With the decreasing small grain size d in BNG, the flow stress is enhanced at first reaching the strongest size at d=14 nm and then experiencing

a mild softening with the continuous decrease of d. The inset figure shows the normalized flow stress, softening rate, of BNG structures compared with that of HNG structures. As is illustrated, the softening rate of HNG structures is decreasing more severely than that of HNG structures, indicating that the strength softening is suppressed in BNG structures. The flow stresses for large grains and small grains in BNG structures are shown in Figure 2.2d.

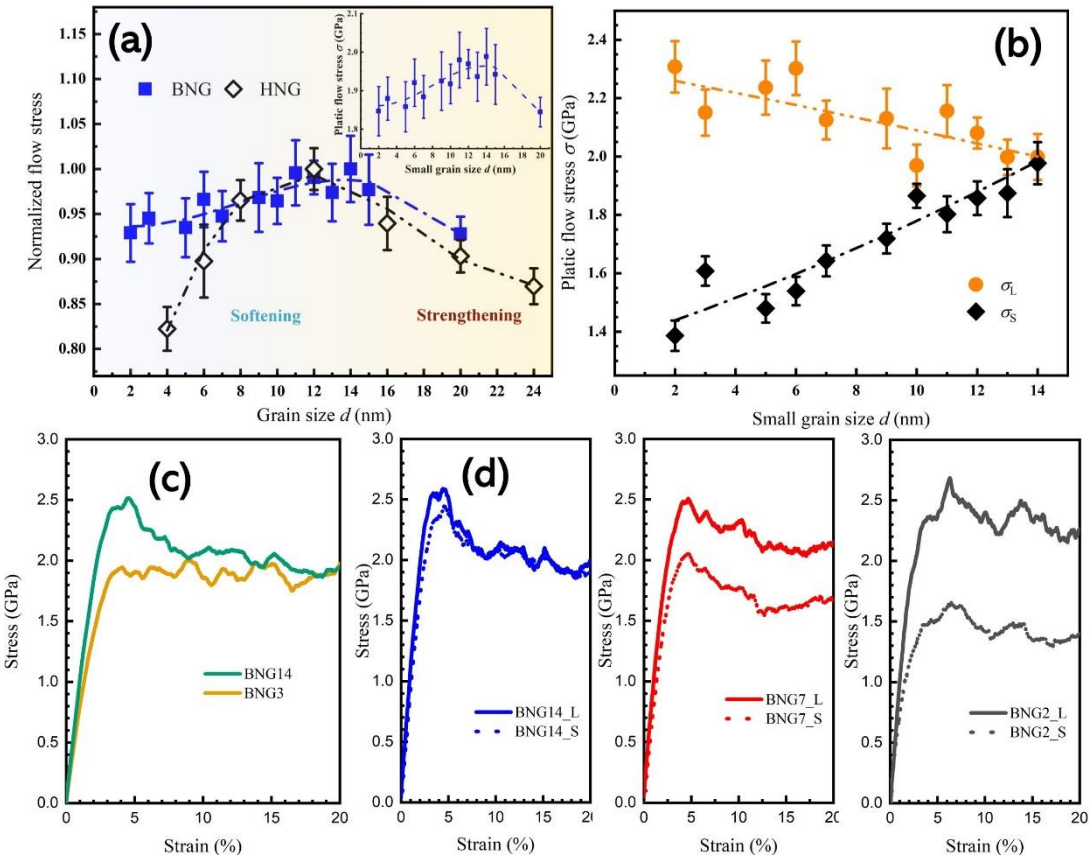

Figure 2.2 | Mechanical properties of bimodal structured Cu. The calculated average plastic flow stress from 10 % to 20 % for a) BNG structures and for b) the corresponding large and small grains in BNG structures respectively. The inset in (a) is the strength softening rate of BNG structures compared with HNG structures. The strain-stress curves of (c) BNG structures with small grain size of 3 nm and 14 nm and of (d) the large and small grains in BNG structures with small grain sizes of 14 nm, 7 nm, and 2 nm respectively.

Due to the grain size effect, the stress in small grains is decreasing constantly with the decrease of d. However, it surprisingly shows an enhanced stress in large grains. The competing process of the decreasing stress in small grains and the enhancing stress in large

grains is responsible for the mediated softening rate of BNG structures. The strain-stress curves (SSC) for 20 nm HNG and BNGs with small grain sizes of 3 nm and 14 nm are portrayed in Figure 2.2e. It is depicted that the SSCs of BNG14 and HNG20 both exhibit a bump after the elastic regime whereas the SSC of BNG3 is more flattened. This is because with the decreasing small grain size, the grain boundaries can better accommodate the plastic deformation, suggesting a transition of mechanism from dislocation mediated plastic deformation to grain boundary mediated plastic deformation[27]. Figure 2.2f shows the SSCs of small grain and large grain in BNG structures with small grain size of 14 nm, 7 nm, and 2 nm respectively. It is obvious that the two curves are deviating from each other with the decrease of d, exhibiting the same trend in Figure 5d.

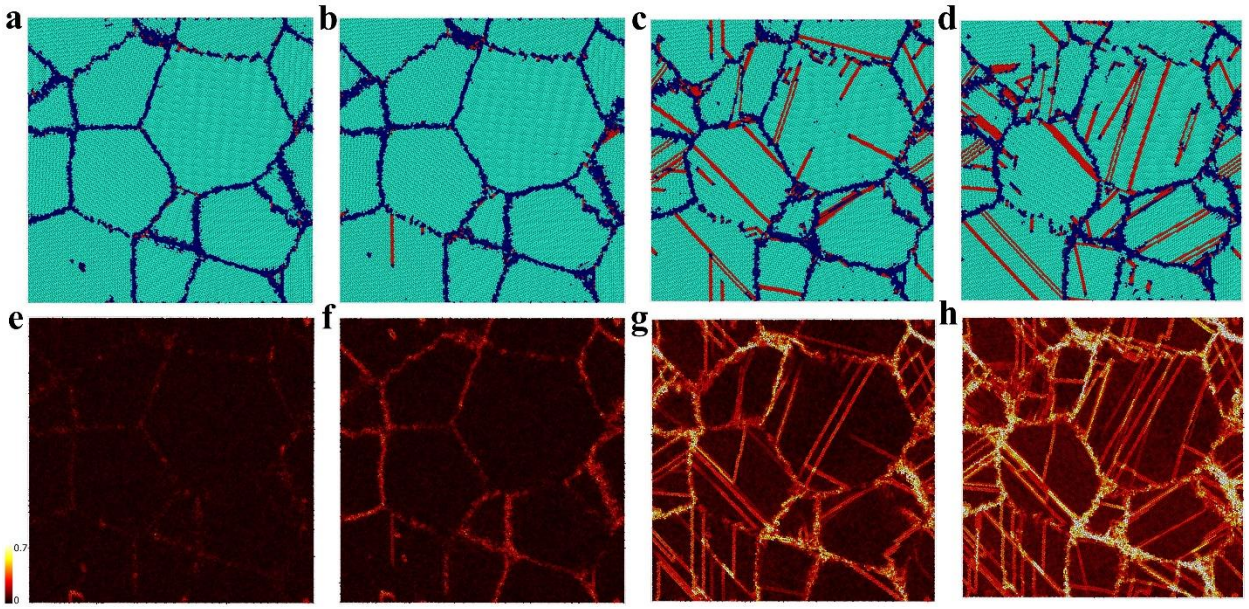

Figure 2.3 | Structure evolution during uniaxial deformation . Deformed BNG structure with small grain size of 14 nm at (a) 1 %, (b) 3 %, (c) 8 %, and (d) 13 % applied strain and the atomic shear strain at (e) 1 %, (f) 3 %, (g) 8 %, and (h) 1 3% applied strain

To disclose how the BNG structure evolves while subjected to the applies strain, Figure 2.3 shows the deformed BNG structure with small grain size of 14 nm at 1%, 3%, 8%, and 13% applied strain and its corresponding spatial distribution of atomic shear strain.

Upon yielding, dislocations are emitting from the grain boundaries of large grains as shown in Figure 2.3b, indicating that the large grains will plastically deform first. From Figure 2.3c and 2.3d, it is obvious that after yielding the severe plastic flips accommodates the further deformation and relax the whole structure, which leads to the drop of stress as shown in Figure 2.2c. However, Figure 2.3a-2.3d are just instantaneous snapshots of the structure, it cannot capture all the ongoing deformation activities. Thus, Figure 2.3e-2.3h illustrate the accumulated slip paths of the structure. As shown in Figure 2.3g and 2.3h, there are slips in the large grains and this means the plastic deformation is mostly governed by large grains.

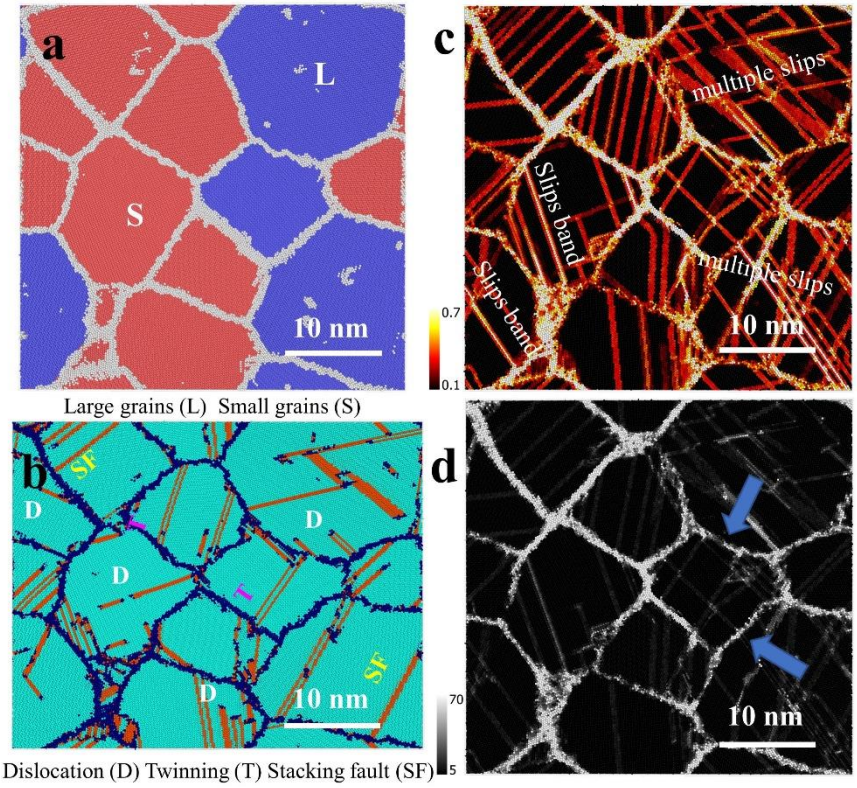

Figure 2.4 | Deformation mechanisms of bimodal structured Cu with small grain size of 14 nm . (a) the BNG structure with small grain size of 14 nm after annealing. The deformation mechanisms at 15 % applied strain shown as (b) deformed structure, (c) local atomic shear strain, and (d) the nonaffine squared displacement.

To exemplify the detailed deformation mechanisms underlying the unprecedented strength softening, here we present the schematics of the strongest BNG structures with

small grain size of 14 nm at 15% applied strain, shown by Figure 2.4a-2.4d. Figure 2.4a illustrates the original configuration of the grain distribution after annealing. The blue regime represents the large grains and the red regime represents the small gains. As shown in Figure 2.4b, deformation mechanisms like dislocation gliding, twinning, and stacking fault are triggered. However, due to the dynamic deformation process, the structures are undergoing drastic defect accumulation and annihilation. Thus, it's unlikely to capture all the ongoing activities within one instantaneous snapshot of the structures. What's more, because of the intrinsic heterogeneity of the grain and grain boundary structures, how they accommodate plastic deformation vary accordingly. Unlike dislocation slip, twinning, and stacking fault induced within grains that can be describe by linear strain field, grain boundary activities such as grain boundary sliding, and migration are more of a nonaffine atomic rearrangement[28][29][30]. As a result, we characterize BNG structures in such way that

$$\boldsymbol{d}_{ij} = \mathbf{J}_i \boldsymbol{d}_{ij}^0 + \delta \boldsymbol{d}_{ij} \tag{1}$$

where $\boldsymbol{d}_{ij}$ is the distant vector from atom *i* to its neighbor atom *j* in the current state and $\boldsymbol{d}_{ij}^0$ represents the initial state. $\mathbf{J}_i$ is an affine transformation tensor that describes linear deformation like dislocation slip, and $\delta \boldsymbol{d}_{ij}$ captures nonaffine atomic rearrangement. $\mathbf{J}_i$ is obtained by taking the minimum of

$$\boldsymbol{D}_i^2 = \sum_{j=1}^{n_i} \left| \boldsymbol{d}_{ij} - \mathbf{J}_i \boldsymbol{d}_{ij}^0 \right|^2 \tag{2}$$

where n_i is the number of neighboring atoms around atom *i*. By this, the atomic shear strain η which captures the plastic slip in the grain interior can be obtained, and by minimizing $\boldsymbol{D}_i^2$,

it can precisely characterize the nonaffine grain boundary activities. Figure 2.4c exhibits the spatial distribution of atomic shear strain η in BNG structure with small grain size of 14 nm at 15% applied strain. The brighter lines in the grain interior are caused by more than one dislocation gliding through the grain forming a typical slip band. It is noteworthy that slips in small grains are mostly parallel to each other, whereas there are more cross slips happening in large grains. This means multiple slip systems are triggered in large grains, indicating the domination of dislocation mediated plastic deformation in large grain regime. The grain boundary activities captured by nonaffine squared displacement $\boldsymbol{D}_i^2$ at the same state as Figure 2.4c are shown in Figure 2.4d. The variations of the white and grey areas exhibit different degrees of grain boundary activity performance. It is depicted that the small grain regime is undergoing severer grain boundary activities compared with large grain regime (arrows), inducing an enhanced plasticity in the large grains.

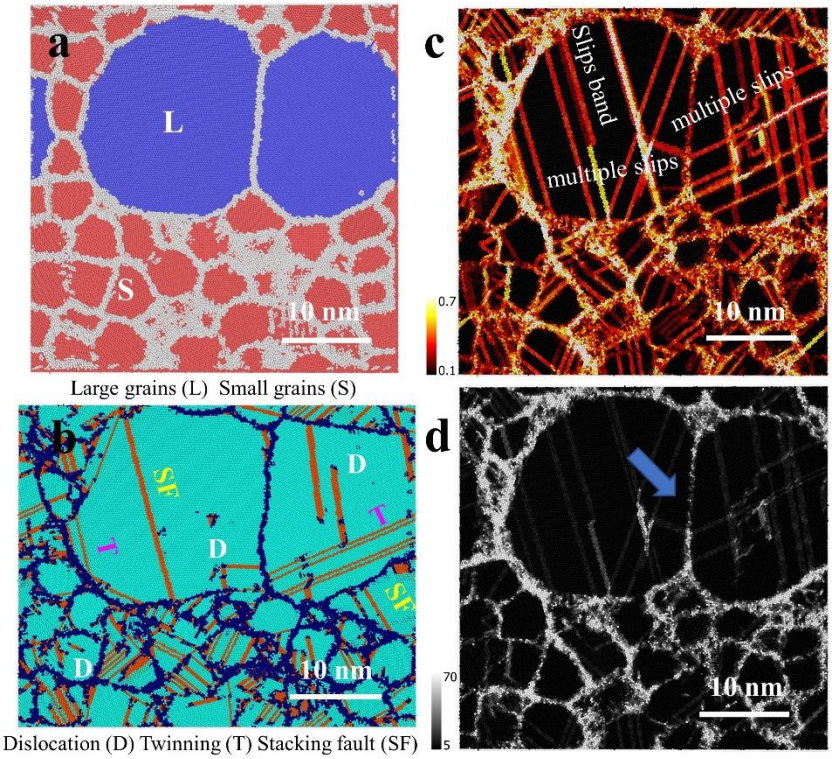

Figure 2.5 | Deformation mechanisms of bimodal structured Cu with small grain size of 6 nm . (a) the BNG structure with small grain size of 6 nm after annealing. The

deformation mechanisms at 15 % applied strain shown as (b) deformed structure, (c) local atomic shear strain, and (d) the nonaffine squared displacement.

What's more, to investigate BNG structure with smaller small grain size, the deformation mechanisms of a typical BNG structure with small grain size of 6 nm is also analyzed in Figure 2.5a-2.5d. Compared with Figure 2.5b and 2.5c, the same deformation qualities are also exhibited in BNG structure with small grain size of 6 nm as shown in Figure 2.5d and 2.5c. However, in Figure 2.5d which maps the spatial distribution of nonaffine squared displacement, the small grain regime does not experience severer grain boundary activities as expected. This identification suggests that the grain boundaries of small grains are stabilized by the unique bimodal grain size distribution, which might explain the alleviation of the strength softening rate.

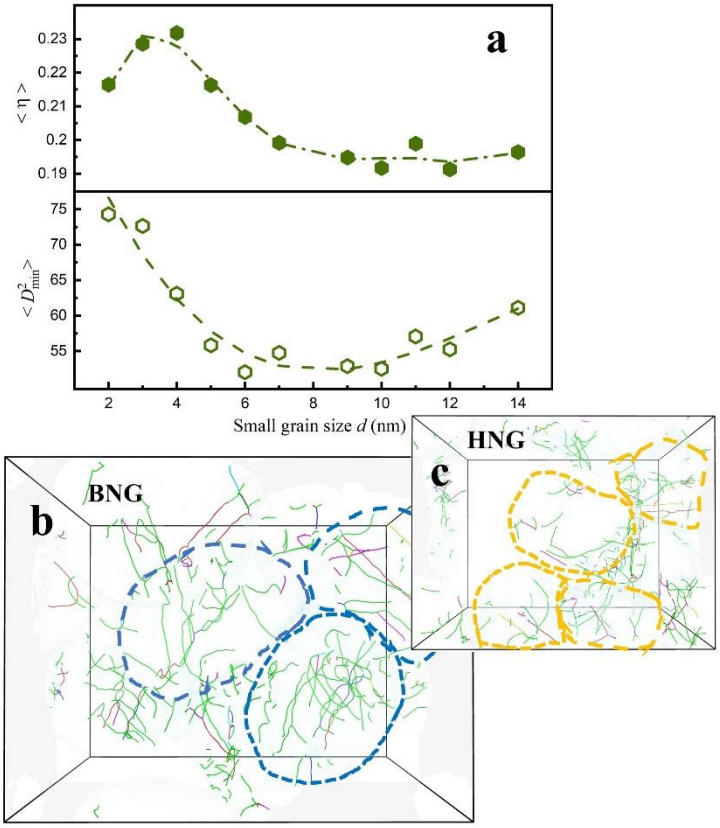

Figure 2.6 | (a) The nonaffine squared displacement $< \boldsymbol{D}^2_{min} >$ and atomic shear strain < η > plotted as a function of small grain size *d* at 15 % applied strain. (b) the dislocation

distribution in 20 nm large grains of BNG structure with small grain size of 2 nm at 20 % applied strain, compared with (d) 20 nm HNG at 20 % applied strain.

To further disclose how the decrease of small grain size *d* affects the plastic slip and grain boundary activities, the atomic shear strain < η > and nonaffine squared displacement $< \boldsymbol{D}^2_{min} >$ are investigated and plotted as a function of small grain size *d* as shown in Figure 2.6a. With the decreasing *d*, the atomic shear strain < η > first increases after the plain segment and then starts to drop when *d* is less than 4 nm. The increasing < η > is induced by the enhanced plasticity in the large grains which corresponds to the increasing plastic flow stress of large grains in Figure 2.2b. Later on, the increasing < η > of large grains yields to the decreasing < η > of small grains and then causes the drop of overall < η >. On the contrary, the nonaffine squared displacement $< \boldsymbol{D}^2_{min} >$ first decreases and then starts to increase when the small grains size *d* is less than 6 nm, indicating that with the decrease of small grain size *d*, the grain boundaries are first stabilized, leading to less grain boundary activities, and then yields to the softening effect of the small grains. In a nutshell, while decreasing the small grain size *d* of BNG, the structure will first experience enhanced plasticity and stabilized grain boundaries but then surrender to the softening effect of the small grains with the continuous decreasing of the small grain size *d*. What's more, Figure 2.6b shows the dislocation distribution of the large grains in BNG with small grain size of 2 nm at 20% applied strain. In order to show a clearer dislocation distribution of large grains, all the small grains are removed and at least two large grains (blue circles) are exposed without overlapping with other grains. Figure 2.6c shows the dislocation distribution of HNG (orange circles) with the same grain size as the large grains in Figure 9b at 20% applied strain and the structure is also modified under the same condition as Figure 9b. From the comparison,

it is clear that there is more dislocation generated in the large grains of BNG structure confirming the enhanced plasticity in large grains, and this also co-relates to the experimental results[14].

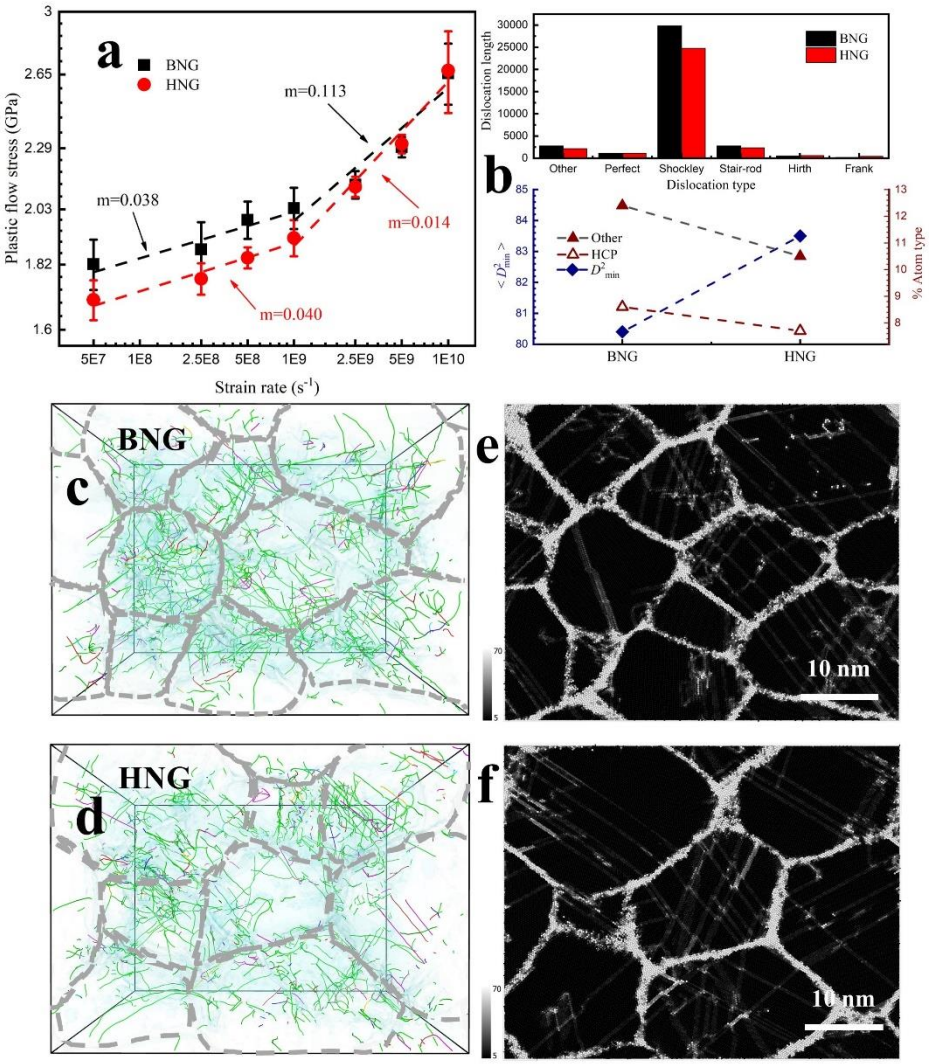

Figure 2.7 | Strain rate effect on BNG Cu . (a) the BNG structure with small grain size of 6 nm after annealing. The deformation mechanisms at 15 % applied strain shown as (b) deformed structure, (c) local atomic shear strain, and (d) the nonaffine squared displacement.

Investigation on strain rate changes is one of the key processes to reveal the deformation mechanisms of metal[31][32], from which the strain rate sensitivity *m* can be calculated and defined by

$$m = \frac{\partial ln\sigma}{\partial ln\dot{\varepsilon}} \quad (2)$$

Figure 2.7a shows the plastic flow stress changes with respect to the variation of strain rate for 20 nm HNG structure and BNG structure with small grain size of 14 nm. By comparing the values of strain rate sensitivity *m*, it is obvious that the BNG structure is less sensitive to strain rate changes than the HNG structure so that the flow stress drop of the BNG structure is less than that of the HNG structure at the same scale of strain rate change. However, previous studies have stated that with the decrease of mean grain size, there will be an increase of strain rate sensitivity[31][33]. To elucidate the surprising strain rate sensitivity of BNG, the total lengths of different dislocation types and the percentages of different atom types in the BNG and HNG structures deformed at 5×10^7 s^{-1} are compared in Figure 2.7b, and Figure 2.7c and 2.7d illustrate the detailed dislocation distribution in the BNG and HNG structures respectively. As the key dislocation types that govern plastic slip, the total length of Shockley partial dislocation[34] and the total length of stair-rod dislocation[4] that is formed by two Shockley partial dislocations meeting and blocking each other are both higher in the BNG structure, which is responsible for the excessive strength of the BNG structure compared with the HNG structure. By analyzing the structure types of each atom, defects such as dislocation, twinning, and stacking fault can be characterized by HCP atom type and grain boundaries otherwise will be categorized to Other atom type due to the amorphous state. As a result, unlike the HNG structure, the fact that the percentage of HCP atom type is higher in the BNG structure also explains why there is no sharp drop with even a smaller mean grain size. It is noteworthy that the percentage of Other atom type which represents grain boundary atoms is also higher in BNG , meaning the grain boundaries take a larger portion of volume in the BNG structure compared with that of the HNG

structure. Figure 2.7c and 2.7d map the spatial distribution of nonaffine squared displacement $< \boldsymbol{D}_{min}^2 >$ for the BNG and HNG structures respectively. It is obvious that the grain boundaries in the HNG structure are in brighter color than that of the BNG structure, suggesting severer grain boundaries activities. This can also be confirmed by the calculated average $< \boldsymbol{D}_{min}^2 >$ values in Figure 2.7b. As a result, even though grain boundaries take a greater portion of volume in the BNG structure, it is still experiencing less grain boundary activities than the HNG structure, indicating the stabilized grain boundaries and the localized plastic deformation in the large grains by the unprecedented bimodal structure[14].

Chapter 3 Summary and Conclusions

This study manifests the effect of grain size ratio on the mechanical behavior of bimodal nanograined structures. It is found that the alleviated softening rate of BNG in inverse Hall-Petch regime is induced by the enhanced plasticity of large grains and alleviated intergranular grain boundary activities. Dislocation mediated deformation mechanisms are believed to contribute the most to the strengthening of nanograined structures[35]. During deformation, dislocation pile-up will be formed at the vicinity of grain boundaries, causing stress concentration at the end of dislocation pile-up. At the same time, a back-stress will be produced pointing the dislocation source. When the stress concentration at grain boundary accumulates to the threshold value of triggering the slip system in the neighboring grains, the grain will then yield to a compromised plasticity. With the decrease of grain size, it will be more reluctant to trigger the slip systems in the grains, which is also known as grain boundary strengthening[36]. Thus, the decreasing size of the neighboring grains around the large grains will give rise to the increase of back-stress so that the large grains can accommodate further deformation. J. Bach and et al[14]. also suggested that thermally activated annihilation of dislocations at grain boundaries for large grains is the dominating deformation mechanism for the BNG structures, and the additional dislocation can be stored at the grain boundaries in order to keep the compatibility of the material, thus, by which the recovery processes of dislocation at the grain boundaries might also be hindered. Our results on the understanding of suppressed softening rate in inverse Hall-Petch effect for the BNG structures shed light on the understanding of the fundamental deformation mechanisms for

emergent heterogeneous structures and guide the improvement of strength-ductility synergy.

Reference

[1] Z. C. Cordero, B. E. Knight, and C. A. Schuh, "Six decades of the Hall–Petch effect – a survey of grain-size strengthening studies on pure metals," *Int. Mater. Rev.*, vol. 61, no. 8, pp. 495–512, 2016, doi: 10.1080/09506608.2016.1191808.

[2] C. E. Carlton and P. J. Ferreira, "What is behind the inverse Hall-Petch effect in nanocrystalline materials?," *Acta Mater.*, vol. 55, no. 11, pp. 3749–3756, Jun. 2007, doi: 10.1016/j.actamat.2007.02.021.

[3] T. J. Rupert, D. S. Gianola, Y. Gan, and K. J. Hemker, "Experimental observations of stress-driven grain boundary migration," *Science (80-.).*, vol. 326, no. 5960, pp. 1686–1690, 2009, doi: 10.1126/science.1178226.

[4] V. Yamakov, D. Wolf, S. R. Phillpot, and H. Gleiter, "Dislocation-dislocation and dislocation-twin reactions in nanocrystalline Al by molecular dynamics simulation," *Acta Mater.*, vol. 51, no. 14, pp. 4135–4147, 2003, doi: 10.1016/S1359-6454(03)00232-5.

[5] A. Rajabzadeh, F. Mompiou, M. Legros, and N. Combe, "Elementary mechanisms of shear-coupled grain boundary migration," *Phys. Rev. Lett.*, vol. 110, no. 26, pp. 1–5, 2013, doi: 10.1103/PhysRevLett.110.265507.

[6] S. L. Thomas, K. Chen, J. Han, P. K. Purohit, and D. J. Srolovitz, "Reconciling grain growth and shear-coupled grain boundary migration," *Nat. Commun.*, vol. 8, no. 1, pp. 1–12, 2017, doi: 10.1038/s41467-017-01889-3.

[7] E. Ma and T. Zhu, "Towards strength–ductility synergy through the design of heterogeneous nanostructures in metals," *Mater. Today*, vol. 20, no. 6, pp. 323–331, 2017, doi: 10.1016/j.mattod.2017.02.003.

[8] P. Cao, "The Strongest Size in Gradient Nanograined Metals," *Nano Lett.*, vol. 20, no. 2, pp. 1440–1446, 2020, doi: 10.1021/acs.nanolett.9b05202.

[9] Y. Wang, M. Chen, F. Zhou, and E. Ma, "High tensile ductility in a nanostructured metal," *Nature*, vol. 419, no. 6910, pp. 912–915, 2002, doi: 10.1038/nature01133.

[10] Y. Zhao *et al.*, "High tensile ductility and strength in bulk nanostructured nickel," *Adv. Mater.*, vol. 20, no. 16, pp. 3028–3033, 2008, doi: 10.1002/adma.200800214.

[11] N. Tsuji, Y. Ito, Y. Saito, and Y. Minamino, "Strength and ductility of ultrafine grained aluminum and iron produced by ARB and annealing," *Scr. Mater.*, vol. 47, no. 12, pp. 893–899, 2002, doi: 10.1016/S1359-6462(02)00282-8.

[12] X. Wu and Y. Zhu, "Heterogeneous materials: a new class of materials with unprecedented mechanical properties," *Mater. Res. Lett.*, vol. 5, no. 8, pp. 527–532, 2017, doi: 10.1080/21663831.2017.1343208.

[13] Y. Zhao, Y. Zhu, and E. J. Lavernia, "Strategies for improving tensile ductility of bulk nanostructured materials," *Adv. Eng. Mater.*, vol. 12, no. 8, pp. 769–778, 2010, doi:

10.1002/adem.200900335.

[14] J. Bach, M. Stoiber, L. Schindler, H. W. Höppel, and M. Göken, "Deformation mechanisms and strain rate sensitivity of bimodal and ultrafine-grained copper," *Acta Mater.*, vol. 186, pp. 363–373, 2020, doi: 10.1016/j.actamat.2019.12.044.

[15] J. Schiøtz, F. D. Di Tolla, and K. W. Jacobsen, "Softening of nanocrystalline metals at very small grain sizes," *Nature*, vol. 391, no. 6667, pp. 561–563, 1998, doi: 10.1038/35328.

[16] I. Lonardelli, J. Almer, G. Ischia, C. Menapace, and A. Molinari, "Deformation behavior in bulk nanocrystalline-ultrafine aluminum: in situ evidence of plastic strain recovery," *Scr. Mater.*, vol. 60, no. 7, pp. 520–523, 2009, doi: 10.1016/j.scriptamat.2008.11.045.

[17] X. Wu *et al.*, "Heterogeneous lamella structure unites ultrafine-grain strength with coarse-grain ductility," *Proc. Natl. Acad. Sci. U. S. A.*, vol. 112, no. 47, pp. 14501–14505, 2015, doi: 10.1073/pnas.1517193112.

[18] J. Sun *et al.*, "A novel process to obtain lamella structured low-carbon steel with bimodal grain size distribution for potentially improving mechanical property," *Mater. Sci. Eng. A*, vol. 785, no. March, p. 139339, 2020, doi: 10.1016/j.msea.2020.139339.

[19] L. Ke, "Making strong nanomaterials ductile with gradients," *Science (80-.).*, vol. 345, no. 6203, pp. 1455 LP – 1456, 2014.

[20] N. Copper, T. H. Fang, W. L. Li, N. R. Tao, and K. Lu, "Tensile Plasticity in Gradient," *Science (80-.).*, vol. 331, no. March, pp. 1587–1590, 2011.

[21] Z. Zeng, X. Li, D. Xu, L. Lu, H. Gao, and T. Zhu, "Gradient plasticity in gradient nano-grained metals," *Extrem. Mech. Lett.*, vol. 8, pp. 213–219, 2016, doi: 10.1016/j.eml.2015.12.005.

[22] M. A. Groeber and M. A. Jackson, "Groeber and Jackson Integrating Materials and Manufacturing Innovation," vol. 3, p. 5, 2014.

[23] S. M. Foiles, M. I. Baskes, and M. S. Daw, "Embedded-atom-method functions for the fcc metals Cu, Ag, Au, Ni, Pd, Pt, and their alloys," *Phys. Rev. B*, vol. 33, no. 12, pp. 7983–7991, 1986, doi: 10.1103/PhysRevB.33.7983.

[24] S. Nosé, "A molecular dynamics method for simulations in the canonical ensemble," *Mol. Phys.*, vol. 52, no. 2, pp. 255–268, 1984, doi: 10.1080/00268978400101201.

[25] W. G.Hoover, "Canonical dynamics: Equilibrium phase-space distributions," *Phys. Rev. A*, vol. 31, no. 1695, 1985, doi: 10.1007/BF00419952.

[26] H. J. C. Berendsen, J. P. M. Postma, W. F. Van Gunsteren, A. Dinola, and J. R. Haak, "Molecular dynamics with coupling to an external bath," *J. Chem. Phys.*, vol. 81, no. 8, pp. 3684–3690, 1984, doi: 10.1063/1.448118.

[27] J. Hu, Y. N. Shi, X. Sauvage, G. Sha, and K. Lu, "Grain boundary stability governs

hardening and softening in extremely fine nanograined metals," *Science (80-.).*, vol. 355, no. 6331, pp. 1292–1296, 2017, doi: 10.1126/science.aal5166.

[28] F. Shimizu, S. Ogata, and J. Li, "Theory of shear banding in metallic glasses and molecular dynamics calculations," *Mater. Trans.*, vol. 48, no. 11, pp. 2923–2927, 2007, doi: 10.2320/matertrans.MJ200769.

[29] C. C. Wang *et al.*, "Real-time, high-Resolution study of nanocrystallization and fatigue cracking in a cyclically strained metallic glass," *Proc. Natl. Acad. Sci. U. S. A.*, vol. 110, no. 49, pp. 19725–19730, 2013, doi: 10.1073/pnas.1320235110.

[30] P. Cao, M. P. Short, and S. Yip, "Understanding the mechanisms of amorphous creep through molecular simulation," *Proc. Natl. Acad. Sci. U. S. A.*, vol. 114, no. 52, pp. 13631–13636, 2017, doi: 10.1073/pnas.1708618114.

[31] Q. Wei, S. Cheng, K. T. Ramesh, and E. Ma, "Effect of nanocrystalline and ultrafine grain sizes on the strain rate sensitivity and activation volume: Fcc versus bcc metals," *Mater. Sci. Eng. A*, vol. 381, no. 1–2, pp. 71–79, 2004, doi: 10.1016/j.msea.2004.03.064.

[32] T. Zhang, K. Zhou, and Z. Q. Chen, "Strain rate effect on plastic deformation of nanocrystalline copper investigated by molecular dynamics," *Mater. Sci. Eng. A*, vol. 648, pp. 23–30, 2015, doi: 10.1016/j.msea.2015.09.035.

[33] J. Chen, L. Lu, and K. Lu, "Hardness and strain rate sensitivity of nanocrystalline Cu," *Scr. Mater.*, vol. 54, no. 11, pp. 1913–1918, 2006, doi: 10.1016/j.scriptamat.2006.02.022.

[34] J. Wang and H. Huang, "Shockley partial dislocations to twin: Another formation mechanism and generic driving force," *Appl. Phys. Lett.*, vol. 85, no. 24, pp. 5983–5985, 2004, doi: 10.1063/1.1835549.

[35] X. Li, Y. Wei, W. Yang, and H. Gao, "Competing grain-boundary- and dislocation-mediated mechanisms in plastic strain recovery in nanocrystalline aluminum," *Proc. Natl. Acad. Sci. U. S. A.*, vol. 106, no. 38, pp. 16108–16113, 2009, doi: 10.1073/pnas.0901765106.

[36] N. Hansen, "Hall-petch relation and boundary strengthening," *Scr. Mater.*, vol. 51, no. 8 SPEC. ISS., pp. 801–806, 2004, doi: 10.1016/j.scriptamat.2004.06.002.